0026-895X/07/7104-1075–1088$20.00
MOLECULAR PHARMACOLOGY
Copyright © 2007 The American Society for Pharmacology and Experimental Therapeutics
Mol Pharmacol 71:1075–1088, 2007

Vol. 71, No. 4
31146/3188360
Printed in U.S.A.

Voltage-Sensitive Oxonol Dyes Are Novel Large-Conductance Ca^{2+}-Activated K^+ Channel Activators Selective for β1 and β4 but Not for β2 Subunits

Takashi Morimoto, Kazuho Sakamoto, Hiroko Sade, Susumu Ohya, Katsuhiko Muraki, and Yuji Imaizumi

Department of Molecular & Cellular Pharmacology, Graduate School of Pharmaceutical Sciences, Nagoya City University, Nagoya, Japan (T.M., K.S., H.S., S.O., Y.I.); and Cell Signaling & Ion Channel Research Group, Cellular Pharmacology, School of Pharmacy, Aichigakuin University, Nagoya, Japan (K.M.)

Received September 23, 2006; accepted January 3, 2007

ABSTRACT

The large-conductance Ca^{2+}-activated K^+ (BK) channel is activated by both the increase of intracellular Ca^{2+} concentration and membrane depolarization. The BK channel plays crucial roles as a key molecule in the negative feedback mechanism regulating membrane excitability and cellular Ca^{2+} in various cell types. Here, we report that a widely used slow-response voltage-sensitive fluorescent dye, bis(1,3-dibutylbarbituric acid)trimethine oxonol [$DiBAC_4(3)$], is a potent BK channel activator. The application of $DiBAC_4(3)$ at concentrations of 10 nM and higher significantly increased whole-cell BK channel currents in human embryonic kidney 293 cells expressing rat BK channel α and β1 subunits (rBK$\alpha\beta$1). In the presence of 300 nM $DiBAC_4(3)$, the activation voltage of the BK channel current shifted to the negative direction by approximately 30 mV, but the single-channel conductance was not affected. $DiBAC_4(3)$ activated whole-cell rBK$\alpha\beta$1 and rBK$\alpha\beta$4 currents in the same concentration range but partially blocked rBK$\alpha\beta$2 currents. The BK channel α subunit alone and some other types of K^+ channels examined were not markedly affected by 1 μM $DiBAC_4(3)$. Structure-activity relationship analyses revealed that a set of oxo- and oxoanion-moieties in two 1,3-dialkylbarbituric acids, which are conjugated by oligomethine, is the novel skeleton for the β-subunit-selective BK channel-opening property of $DiBAC_4(3)$ and related oxonol compounds. This conjugated structure may be located stereochemically in one plane. These findings provide a molecular and structural basis for understanding the regulatory mechanism of BK channel activity by an auxiliary β subunit and will be fundamental to the development of β-selective BK channel openers.

The large-conductance Ca^{2+}-activated voltage-gated K^+ (BK) channel is activated by both the increase in intracellular Ca^{2+} concentration ($[Ca^{2+}]_i$) and membrane depolarization (Vergara et al., 1998). BK channels are functionally expressed in a wide variety of excitable cells as key molecules in the negative feedback mechanisms in $[Ca^{2+}]_i$ regulation. BK channels are composed of tetrametric sets consisting of a pore-forming α subunit and an auxiliary β subunit (Wallner et al., 1996). The α subunit has a characteristic extracellular N-terminal region coupled with the β subunit, seven transmembrane segments, and a long intracellular C-terminal region essential for Ca^{2+} sensing and tetramerization (Schre-

This work was supported by a Grant-in-Aid for Scientific Research on Priority Areas (18059029) from the Ministry of Education, Culture, Sports, Science, and Technology, Japan, and by a Grant-in-Aid for Scientific Research (B) (17390045) from the Japan Society for the Promotion of Science (to Y.I.). This work was also supported by a Grant-in-Aid for Research on Health Sciences focusing on Drug Innovation (KH11001) from the Japan Health Sciences Foundation (to Y.I.).

Article, publication date, and citation information can be found at http://molpharm.aspetjournals.org.

doi:10.1124/mol.106.031146.

ABBREVIATIONS: BK channel, large-conductance Ca^{2+}-activated K^+ channel; SK channel, small-conductance Ca^{2+}-activated K^+ channel, Kv channel, voltage-gated K^+ channel; K_{ATP} channel, ATP-sensitive K^+ channel; AE, anion exchanger; mUBSMC, mouse urinary bladder smooth muscle cell; HEK, human embryonic kidney; BKα, large-conductance Ca^{2+}-activated K^+ channel α subunit; BKβ, large-conductance Ca^{2+}-activated K^+ channel β subunit; BK$\alpha\beta$1, large-conductance Ca^{2+}-activated K^+ channel α plus β1 subunits; BK$\alpha\beta$2, large-conductance Ca^{2+}-activated K^+ channel α plus β2 subunits; BK$\alpha\beta$4, large-conductance Ca^{2+}-activated K^+ channel α plus β4 subunits; r, rat; m, mouse; DHS-I, dehydrosoyasaponin-I, BA, barbituric acid; DMBA, 1,3-dimethylbarbituric acid; DETBA, 1,3-diethyl-2-thiobarbituric acid; DiBAC, bis(1,3-dialkylbarbituric acid)oligomethine oxonol; DiSBAC, bis(1,3-dialkylthiobarbituric acid)oligomethine oxonol; $DiBAC_4(3)$, bis(1,3-dibutylbarbituric acid)trimethine oxonol; $DiBAC_4(5)$, bis(1,3-dibutylbarbituric acid)pentamethine oxonol; $DiSBAC_4(3)$, bis(1,3-dibutylthiobarbituric acid)trimethine oxonol; $DiSBAC_2(3)$, bis(1,3-diethylthiobarbituric acid)trimethine oxonol; $DiSBAC_2(5)$, bis(1,3-diethylthiobarbituric acid)pentamethine oxonol; $DiSBAC_2(1)$, bis(1,3-diethylthiobarbituric acid) methine oxonol; $DiSBAC_0(5)$, bis(barbituric acid)pentamethine oxonol; $DiSBAC_{10}(3)$, bis(1,3-didecylthiobarbituric acid)trimethine oxonol; Oxonol 595, bis(3-cyano-1-ethyl-4-methyl-2,6-dioxo-1,2,5,6-tetrahydropyridine)trimethine oxonol; Oxonol V, bis(3-phenyl-5-oxoisoxazol-4-yl)pentamethine oxonol; Oxonol VI, bis(3-propyl-5-oxoisoxazol-4-yl)pentamethine oxonol; DFT, density-functional theory; NS-1619, 1-(2′-hydroxy-5′-trifluoromethylphenyl)-5-trifluoromethyl-2(3*H*)-benzimidazolone; UCL 1684, 6,10-diaza-3(1,3)8,(1,4)-dibenzena-1,5(1,4)-diquinolinacy clodecaphane.

iber and Salkoff, 1997; Quirk and Reinhart, 2001). The pore-forming α subunit (BKα) is a member of the *slo* family of potassium channels (KCNMA1) originally identified in *Drosophila melanogaster* (Elkins et al., 1986). Only one major type of BKα and several splice variants are expressed ubiquitously in a wide variety of tissues, except heart (Xie and McCobb, 1998; Zarei et al., 2001). In contrast, four different β subunits with tissue-specific distribution have been identified (KCNMB1–4) (Knaus et al., 1994; Wallner et al., 1999; Brenner et al., 2000a; Uebele et al., 2000). These β subunits share a prototypic topology of two transmembrane domains with intracellular N and C termini. Coexpression of β subunits with α subunits dramatically alters the biophysical and pharmacological properties of the α-subunit BK channel, including apparent Ca^{2+} sensitivity, voltage-dependence, gating kinetics, and pharmacological sensitivity, and it contributes to the diversity in BK channel function (McManus et al., 1995; Xia et al., 1999, 2000; Meera et al., 2000; Weiger et al., 2000; Orio et al., 2002; Zeng et al., 2003).

The β1 and β4 subunits are expressed predominantly in smooth muscles and neurons, respectively (Meera et al., 2000; Weiger et al., 2000; Petkov et al., 2001). The smooth-muscle-specific β1 subunit (KCNMB1) increases the BK channel's apparent Ca^{2+}/voltage sensitivity, and its disruption in mice increases arterial tonus and phasic contractions of urinary bladder by the reduction of functional coupling between Ca^{2+} sparks and BK channel activation (Brenner et al., 2000b; Petkov et al., 2001). A deficiency of the α subunit (KCNMA1) in mice can cause not only diseases related to smooth muscle dysfunctions, such as elevated blood pressure, overactive bladder, urinary incontinence, and erectile dysfunction, but also cerebellar ataxia, hearing loss, and hyperaldosteronism (Meredith et al., 2004; Rüttiger et al., 2004; Sausbier et al., 2004, 2005). Therefore, BK channel-openers selectively targeting the β1 subunit may effectively treat overactive smooth muscle disorders with minimal side effects. This is supported by the fact that β-estradiol reduces susceptibility to cardiovascular disease in premenopausal women and by the fact that it activates the BK channel only in the copresence of the β1 subunit (Valverde et al., 1999; Ohya et al., 2005). The gain-of-function variant of the β1 subunit (the E65K mutation) protects against diastolic hypertension in aging women (Fernandez-Fernandez et al., 2004). However, despite the tissue-specific distribution of β subunits, few BK channel openers targeting selective β subunits have been identified, whereas various chemical and endogenous BK channel openers have been characterized as BKα openers (Imaizumi et al., 2002; Nardi et al., 2003).

$DiBAC_4(3)$, a slow-response voltage-sensitive fluorescent dye, and related oxonol derivatives are generally used to screen K_{ATP} channel modulators by fluorometric imaging plate reader (González et al., 1999; Whiteaker et al., 2001) or to assess bacterial viability by flow cytometry (Jepras et al., 1997). We have used $DiBAC_4(3)$ at low concentrations to screen BK channel openers (Yamada et al., 2001) and demonstrated that pimaric acid and related pimarane compounds activate the BK channel by acting on the α subunit (Imaizumi et al., 2002). At that time, we could not determine the opening effect of $DiBAC_4(3)$ on the recombinant BK channel, because 50 nM $DiBAC_4(3)$ was used as a voltage indicator. In recent preliminary studies, we found that the BK$\alpha\beta$1-opening effects of pimaric acid and NS-1619 could not be clearly detected in the presence of $DiBAC_4(3)$ at higher concentrations (> 1 μM), presumably because BK channels were extensively activated by $DiBAC_4(3)$. In this study, we report the pharmacological effects of $DiBAC_4(3)$ and selectivity among the β subunits and selectivity for other K^+ channels by patch-clamp techniques. Using $DiBAC_4(3)$ analogs and structurally related compounds, we determined the essential site in the bis-oxonol structure for β-subunit-dependent activation of BK channels.

Materials and Methods

Cell Isolation. Mouse urinary bladder smooth muscle cells (mUBSMCs) were isolated using a method described previously (Morimura et al., 2006). In brief, the urinary bladder was dissected out from male C57BL/6 mice (8–12 weeks of age), and mUBSMCs were obtained by enzymatic isolation using 0.2% collagenase (Amano Enzyme, Nagoya, Japan) for 11 to 13 min at 37°C.

Transfection and Cell Culture. HEK293 cells were maintained in minimum essential medium (Invitrogen, Carlsbad, CA) supplemented with 10% heat-inactivated fetal bovine serum (Cell Culture Technologies, Buhnrain/Zurich, Switzerland), 100 units/ml penicillin (Wako Pure Chemicals, Osaka, Japan), and 100 μg/ml streptomycin (Meiji Seika, Tokyo, Japan) at 37°C in 5% CO_2 atmosphere. We used HEK293 cell lines that stably expressed rBKα, rSK2, mSK4, rKv1.1, and rKv4.3 (HEK-rBKα, HEK-rSK2, HEK-mSK4, HEK-rKv1.1, and HEK-rKv4.3) and that were generated in previous studies by transfecting the cDNAs encoding rBKα, rSK2, mSK4, rKv1.1, and rKv4.3 in pcDNA3.1(+) (Invitrogen) (Yamada et al., 2001; Imaizumi et al., 2002; Hatano et al., 2004; Sakamoto et al., 2006). HEK293 cell lines stably coexpressing both rBKα and either rBKβ1 or rBKβ4 (HEK-rBK$\alpha\beta$1 and HEK-rBK$\alpha\beta$4) were also generated in the previous studies. HEK293 cells transiently coexpressing both rBKα and rBKβ2 (HEK-rBK$\alpha\beta$2) were generated by cotransfecting the cDNAs encoding both rBKα in pcDNA3.1(+) and rBKβ2 in pTracer-CMV2 (Invitrogen); the transfected cells were identified by green fluorescent protein signals derived from pTracer-CMV2 after 24 to 96 h of cultivation. Transfected cells were maintained on small pieces of cover glass in culture dishes and then were used for electrophysiological experiments.

Electrophysiology. Whole-cell and inside-out patch clamps were applied to single cells using CEZ-2200, CEZ-2300, and CEZ-2400 amplifiers (Nihon Kohden, Tokyo, Japan) and an EPC-7 amplifier (HEKA Electronik, Lambrecht, Germany) in the manner reported previously (Imaizumi et al., 2002). The procedures of electrophysiological recordings and data acquisition/analysis for whole-cell recording were performed by using two programs, Data-Acquisition and Cell-Soft, developed at the University of Calgary (Calgary, AB, Canada). Single-channel current analyses were done using PAT V7.0C software developed at the University of Strathclyde (Glasgow, Scotland, UK). The pipette resistance was 2 to 5 MΩ for the whole-cell and 10 to 15 MΩ for inside-out patch configurations when filled with the pipette solutions.

Solution. For whole-cell recording from isolated mUBSMCs or transfected HEK293 cells, a standard HEPES-buffered solution composed of 137 mM NaCl, 5.9 mM KCl, 2.2 mM $CaCl_2$, 1.2 mM $MgCl_2$, 10 mM HEPES, and 14 mM D-glucose, pH 7.4 by NaOH, was used as a bath solution. Whole-cell patch-clamp recordings in mUBSMCs were obtained using a 300 nM free Ca^{2+} internal pipette solution containing 140 mM KCl, 4.5 mM $CaCl_2$, 3 mM $MgCl_2$, 10 mM EGTA, 10 mM HEPES, and 2 mM ATP, pH 7.2 by KOH, and the standard HEPES-buffered solution, including 100 μM Cd^{2+}. Whole-cell patch-clamp recordings in HEK-rBKα, HEK-rBK$\alpha\beta$1, and HEK-rBK$\alpha\beta$4 were obtained using a 300 nM free Ca^{2+} internal pipette solution containing 140 mM KCl, 3.3 mM $CaCl_2$, 1 mM $MgCl_2$, 5 mM EGTA, 10 mM HEPES, and 2 mM $ATPNa_2$, pH 7.2 by KOH. Whole-cell patch-clamp recording in HEK-rBK$\alpha\beta$2 was performed using a 1 μM

free Ca^{2+} internal pipette solution containing 140 mM KCl, 4.3 mM $CaCl_2$, 4 mM $MgCl_2$, 5 mM EGTA, 10 mM HEPES, and 2 mM $ATPNa_2$, pH 7.2 by KOH. Whole-cell patch-clamp recordings in HEK-rSK2 and HEK-mSK4 were performed using a 1 μM free Ca^{2+} internal pipette solution containing 138 mM potassium aspartate, 8.6 mM $CaCl_2$, 2 mM $MgCl_2$, 10 mM EGTA, 10 mM HEPES, and 1 mM $ATPK_2$, pH 7.2 by KOH. Liquid junction potentials were measured and corrected for −14 mV. Whole-cell patch-clamp recordings in HEK-rKv1.1 and HEK-rKv4.3 were performed using a nominally Ca^{2+}-free (~10 nM) internal pipette solution containing 138 mM KCl, 0.58 mM $CaCl_2$, 2 mM $MgCl_2$, 10 mM EGTA, 10 mM HEPES, and 1 mM $ATPK_2$, pH 7.2 by KOH. For single-channel recording under an inside-out configuration, HEPES-buffered solution composed of 140 mM KCl, 2.2 mM $CaCl_2$, 1.2 mM $MgCl_2$, 5 mM EGTA, 10 mM HEPES, and 14 mM D-glucose (pCa 7.0), pH 7.2 by NaOH, was used as bath and pipette solutions. The free Ca^{2+} concentration was calculated using the WEBMAXC program (http://www.stanford.edu/~cpatton/webmaxcS.htm).

Chemicals. bis(1,3-Dibutylbarbituric acid)trimethine oxonol [DiBAC$_4$(3)] was obtained from Dojindo (Kumamoto, Japan); bis(1,3-dibutylbarbituric acid)pentamethine oxonol [DiBAC$_4$(5)] and bis(1,3-diethylthiobarbituric acid)trimethine oxonol [DiSBAC$_2$(3)] were obtained from Invitrogen (Carlsbad, CA); bis(1,3-diethylthiobarbituric acid)pentamethine oxonol [DiSBAC$_2$(5)]was obtained from AnaSpec, Inc. (San Jose, CA); bis(1,3-diethylthiobarbituric acid) methine oxonol [DiSBAC$_2$(1)] was obtained from Specs, Inc. (Delft, Netherlands); barbituric acid (BA) was obtained from Wako Pure Chemicals; bis(1,3-dibutylthiobarbituric acid)trimethine oxonol [DiSBAC$_4$(3)], bis(barbituric acid)pentamethine oxonol [DiSBAC$_0$(5)], bis(3-cyano-1-ethyl-4-methyl-2,6-dioxo-1,2,5,6-tetrahydropyridine)trimethine oxonol (Oxonol 595), bis(3-phenyl-5-oxoisoxazol-4-yl)pentamethine oxonol (Oxonol V), 1,3-dimethylbarbituric acid (DMBA), 1,3-diethyl-2-thiobarbituric acid (DETBA), and penitrem A were obtained from Sigma-Aldrich (St. Louis, MO); bis(3-propyl-5-oxoisoxazol-4-yl)pentamethine oxonol (Oxonol VI) was obtained from Fluka (Buchs, Switzerland); and bis(1,3-didecylthiobarbituric acid)trimethine oxonol [DiSBAC$_{10}$(3)] was obtained from Cayman Chemical (Ann Arbor, MI). DiBAC$_4$(3), DiBAC$_4$(5), DiSBAC$_2$(3), DiSBAC$_2$(5), DiSBAC$_4$(3), DiSBAC$_0$(5), DiSBAC$_2$(1), Oxonol 595, Oxonol V, Oxonol VI, and penitrem A were diluted from a 10 mM stock in dimethyl sulfoxide; and BA, DMBA, and DETBA were diluted from a 100 mM stock in dimethyl sulfoxide and stored at −20°C. Less soluble compounds were prepared for use in the experiments by sonication to dissolve in a bath solution for almost a minute.

Stereochemical Optimization of Chemical Structure and Calculations of pK_a and Interatomic Distance. The most stable stereochemical structures of oxonol compounds were determined by calculations in the anion state [except for DiSBAC$_0$(5), which forms a dianion by tautomerization] using the density-functional theory (DFT) methods in Spartan '04 software for Windows version 1.0.3. (Wavefunction, Inc., Irvine, CA) and displayed by Chimera software (University of California, San Francisco, San Francisco, CA). Interatomic oxygen-oxygen distances were measured from the most stable stereochemical structures. The pK_a values, determined by the degree of ionization of the molecules, were calculated using Solaris V4.76 software (Advanced Chemistry Development, Inc., Toronto, ON, Canada).

Statistics. Data are expressed as means ± S.E.M. Statistical significance between two groups and among multiple groups was evaluated using the Student's t test and Scheffe's test after the F test or one-way analysis, respectively. In the figures, * and ** indicate statistical significance at p values of 0.05 and 0.01, respectively.

Results

DiBAC$_4$(3) Activates BK Current in Isolated mUBSMCs. In the first part of this study, we examined the effects of DiBAC$_4$(3) on outward currents elicited by depolarization in single smooth muscle cells isolated from mouse urinary bladder (mUBSMCs) by patch-clamp techniques. Whole-cell currents in mUBSMCs upon depolarization were measured in the standard HEPES-buffered solution containing 100 μM Cd^{2+} to block the voltage-dependent Ca^{2+} channel and with the use of a pipette solution, in which the Ca^{2+} concentration was fixed at pCa 6.5 with Ca^{2+}-EGTA buffer (see *Materials and Methods*). The outward currents elicited by depolarization from a holding potential of −60 to +40 mV for 150 ms (● in Fig. 1A) were markedly enhanced by the application of 300 nM DiBAC$_4$(3) and then were blocked by the addition of 1 μM penitrem A, a selective BK channel blocker (Fig. 1A). The outward currents elicited by depolar-

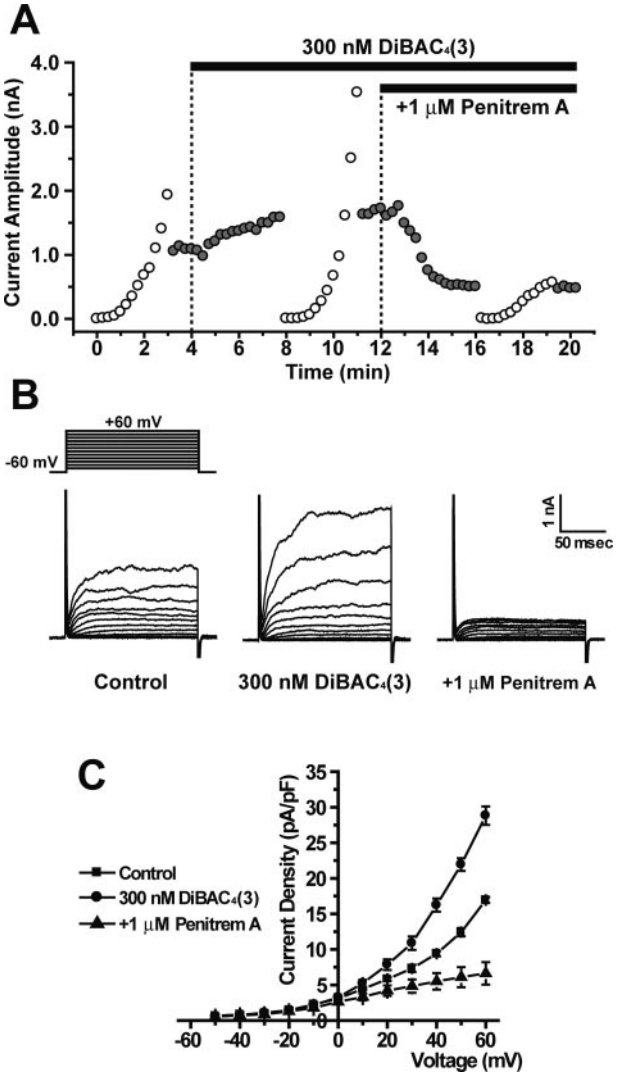

Fig. 1. Effects of DiBAC$_4$(3) on whole-cell BK currents in mUBSMCs. Whole-cell BK currents in mUBSMCs were measured in physiological K^+ gradient conditions (5.9 mM K^+ outside and 140 mM K^+ inside) with 300 nM free Ca^{2+} in the pipette solution (pCa 6.5). A, each cell was depolarized from a holding potential of −60 mV to +60 mV in 10-mV steps (○) or to +40 mV (●) for 150 ms at 15-s intervals. Whole-cell BK currents were measured in the control, in the presence of 300 nM DiBAC$_4$(3), and after the addition of 1 μM penitrem A. The peak amplitude of outward current was plotted against time. Application of 300 nM DiBAC$_4$(3) and addition of 1 μM penitrem A are indicated by horizontal bars, respectively. B, recordings of the outward currents activated by 10-mV steps in A (○) are shown. C, the current-voltage relationships were obtained in the control (■, n = 4), in the presence of 300 nM DiBAC$_4$(3) (●; n = 4), and after the addition of 1 μM penitrem A (▲; n = 4).

ization in the range of −60 to +60 mV in 10-mV steps for 150 ms (○ in Fig. 1A) were recorded (Fig. 1B) and plotted as the relationship between current density and test potentials (Fig. 1C). The peak outward current densities at +60 mV in the control, in the presence of $DiBAC_4(3)$ and after the addition of penitrem A, were 16.9 ± 0.4, 28.8 ± 1.3 ($p < 0.01$ versus the control), and 6.6 ± 1.6 pA/pF ($p < 0.01$ versus in the presence of $DiBAC_4(3)$; $p < 0.05$ versus the control), respectively ($n = 4$ for each). These results suggest that $DiBAC_4(3)$ potently activates BK current in mUBSMCs, in which BK channels consist of combinations of α and β1 subunits (Petkov et al., 2001).

$DiBAC_4(3)$ Is a Novel BK Channel Opener. The effects of $DiBAC_4(3)$ on BK channels were further examined in a heterologous expression system, in which rat BK channel α subunit (rBKα) alone, or both rBKα and either rat BK channel β1, β2, or β4 subunit (rBKβ1, rBKβ2, or rBKβ4) were stably or transiently expressed in HEK293 cells (HEK-rBKα, HEK-rBK$\alpha\beta$1, HEK-rBK$\alpha\beta$2, and HEK-rBK$\alpha\beta$4). First, whole-cell currents in HEK-rBK$\alpha\beta$1 were measured in the standard solution and by using a pipette solution of pCa 6.5. The outward currents elicited by depolarization from a holding potential of −60 mV in 10-mV steps for 150 ms in HEK-rBK$\alpha\beta$1 were markedly enhanced at potentials positive to −40 mV by application of 300 nM $DiBAC_4(3)$ and then were completely blocked by the addition of 1 μM penitrem A (Fig. 2A). The relationships between current density and test potentials are shown in Fig. 2B. The peak outward current densities at +60 mV in the control, in the presence of $DiBAC_4(3)$ and after the addition of penitrem A, were 142.8 ± 14.6, 219.1 ± 35.8 ($p < 0.01$ versus control), and 2.4 ± 2.0 pA/pF [$p < 0.01$ versus the control and in the presence of $DiBAC_4(3)$], respectively ($n = 3$ for each). The cumulative application of $DiBAC_4(3)$ in the concentration range of 10 nM to 1 μM increased the outward currents concentration-dependently at +20 mV in HEK-rBK$\alpha\beta$1. The outward currents were then almost completely blocked by the further addition of 1 μM penitrem A (Fig. 2C). Concentration-response relationships for $DiBAC_4(3)$ in HEK-rBK$\alpha\beta$1 were summarized as the relative amplitude normalized by the peak outward current before the application of $DiBAC_4(3)$ (Fig. 2D). The relative amplitude at +20 mV was concentration-dependently increased by $DiBAC_4(3)$ at 10 nM (1.440 ± 0.242; $p < 0.05$ versus 1.0) and higher concentrations. The effect of $DiBAC_4(3)$ at lower concentration (< 100 nM) was removed by washout within a few minutes and that at higher concentration (> 300 nM) was removed more slowly (data not shown).

Single-channel currents in HEK-rBK$\alpha\beta$1 were measured at +20 mV in the inside-out patch configuration in symmetrical 140 mM K^+ conditions (Fig. 3A). The pCa in the bath and pipette solutions was 7.0 (see *Materials and Methods*). Relative open probability (P_o) was normalized by that before the application of $DiBAC_4(3)$. Cumulative application of $DiBAC_4(3)$ from 100 nM to 3 μM increased the relative P_o of rBK$\alpha\beta$1 channels in a concentration-

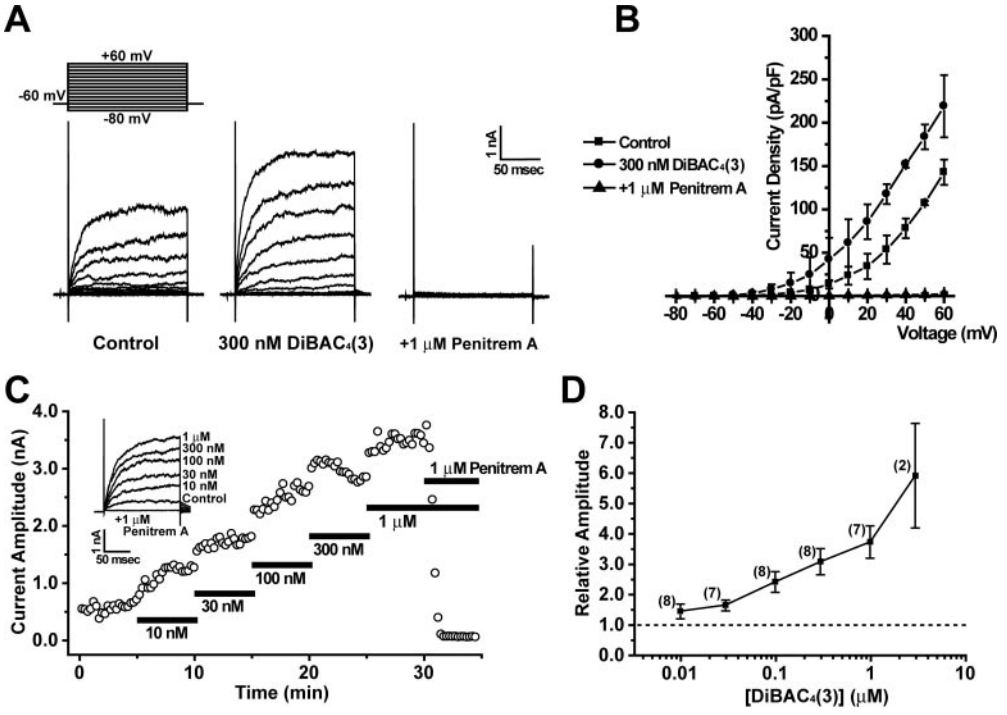

Fig. 2. Effects of $DiBAC_4(3)$ on whole-cell rBK$\alpha\beta$1 currents in HEK293 cells. Whole-cell rBK$\alpha\beta$1 currents were measured in physiological K^+ gradient conditions (5.9 mM K^+ outside and 140 mM K^+ inside) with 300 nM free Ca^{2+} in the pipette solution (pCa 6.5). A, each cell was depolarized from a holding potential of −60 mV to +60 mV in 10-mV steps for 150 ms at 15-s intervals. Whole-cell rBK$\alpha\beta$1 currents were measured in the control, in the presence of 300 nM $DiBAC_4(3)$, and after the addition of 1 μM penitrem A. B, the current-voltage relationships were obtained in the control (■, $n = 3$), in the presence of 300 nM $DiBAC_4(3)$ (●; $n = 3$), and after the addition of 1 μM penitrem A (▲; $n = 3$). C, $DiBAC_4(3)$ was applied cumulatively in the concentration ranges of 10 nM to 1 μM, and then 1 μM penitrem A was further added. Each cell was depolarized from a holding potential of −60 mV to +20 mV (○) for 150 ms at 15-s intervals. The peak outward current amplitude was plotted against time. Original current traces at different concentrations are superimposed and shown in the inset. D, concentration-response relationships of $DiBAC_4(3)$ on whole-cell rBK$\alpha\beta$1 currents (■) were obtained from experiments typically shown in C. The relative amplitudes were obtained by normalizing the peak outward current by that before the application of $DiBAC_4(3)$. The numbers of individual experiments performed are indicated in parentheses.

dependent manner (Fig. 3, A and B). The increase in relative P_o of rBK$\alpha\beta$1 channels by application of DiBAC$_4$(3) could be quickly and completely removed by washout. The concentration-response relationships of DiBAC$_4$(3) on relative P_o are summarized in Fig. 3C. The unitary current amplitude at +50 mV and single-channel conductance were 12.37 ± 0.07 pA, 260.2 pS, and 12.76 ± 0.24 pA, 263.4 pS ($p > 0.05$ versus the control, respectively; $n = 5$ for each) in the absence and presence of 300 nM DiBAC$_4$(3), respectively (Fig. 3D). The P_o was increased by the application of 300 nM DiBAC$_4$(3) at any potential examined and was well-fitted by a Boltzmann relationship: $P_o = 1/[1 + \exp\{(V_{1/2} - V_m)/S\}]$, where $V_{1/2}$, V_m, and S are the voltages required for half-maximum activation, membrane potential, and slope factor, respectively (Fig. 3E). The values of $V_{1/2}$ and S were 96.3 ± 2.7 and 11.4 ± 2.2 mV in the absence of DiBAC$_4$(3), and 74.8 ± 8.4 ($p < 0.01$ versus the control) and 17.3 ± 4.3 mV ($p > 0.05$ versus the control) in the presence of 300 nM DiBAC$_4$(3), respectively ($n = 5$ for each). The fitted line was shifted to negative potentials by approximately 30 mV in the presence of 300 nM DiBAC$_4$(3).

To examine whether the enhancement of rBK$\alpha\beta$1 channel activity by DiBAC$_4$(3) can be observed in different cytosolic

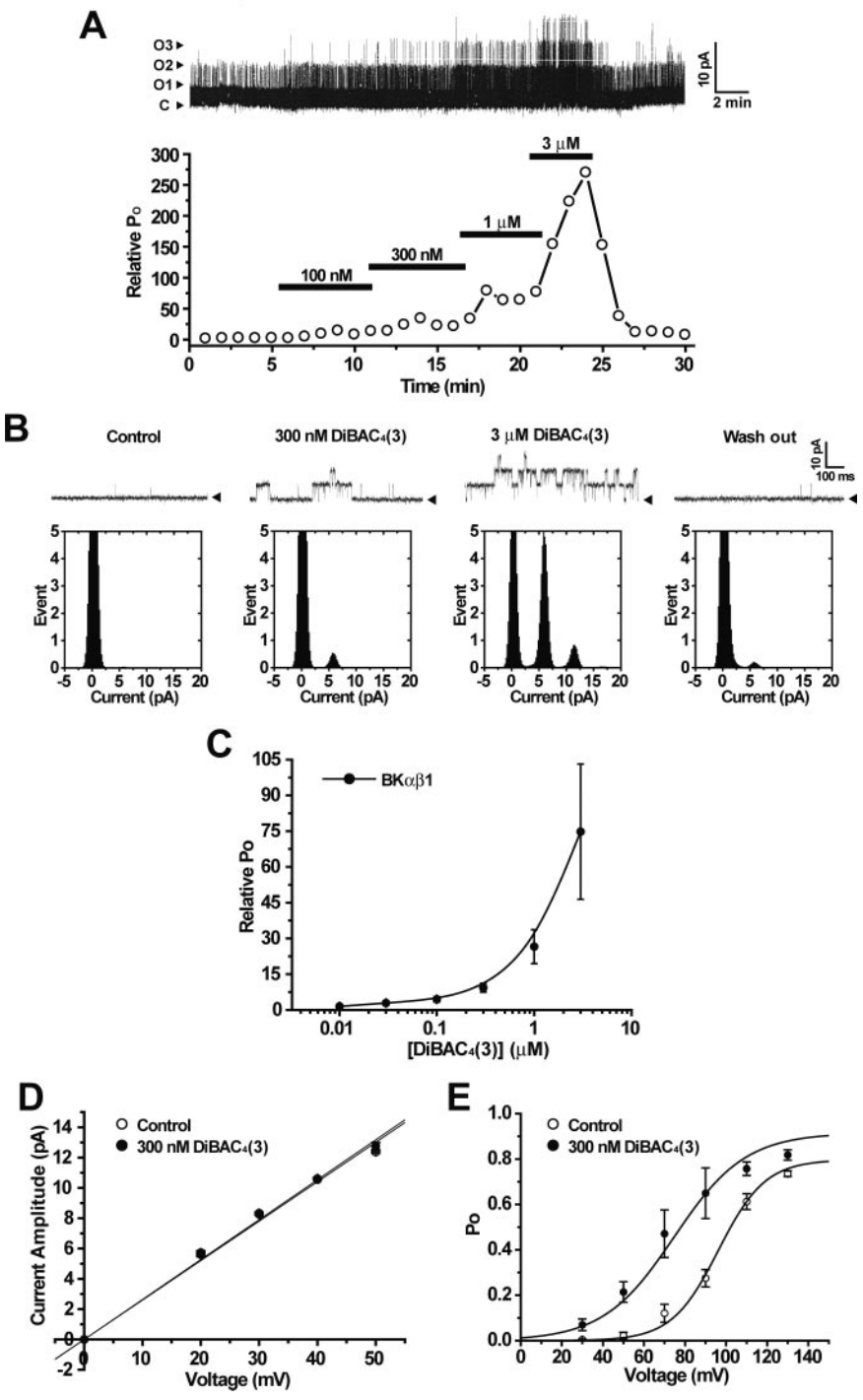

Fig. 3. Effects of DiBAC$_4$(3) on single-channel rBK$\alpha\beta$1 currents in HEK293 cells. A, single-channel rBK$\alpha\beta$1 currents were measured under the inside-out patch configuration in symmetrical 140 mM K^+ conditions with 100 nM free Ca^{2+} in the bath and pipette solution (pCa 7.0) recorded at +20 mV. DiBAC$_4$(3) was applied cumulatively in the concentration ranges of 100 nM to 3 μM and then washed out. Relative P_o was normalized by P_o before the application of DiBAC$_4$(3). C, O1, O2, and O3 indicate closed and open state levels of BK channels, respectively. The increase in relative P_o of rBK$\alpha\beta$1 channels (○) by application of DiBAC$_4$(3) was removed by washout. B, original traces and amplitude histograms in the control, in the presence of 300 nM or 3 μM DiBAC$_4$(3), and after washout were obtained from the recording shown in A. The arrowhead indicates the closed state level of BK channels. C, concentration-response relationships of DiBAC$_4$(3) on relative P_o of rBK$\alpha\beta$1 channels (●; $n = 4$) were obtained from experiments shown in A. D, single-channel rBK$\alpha\beta$1 currents were recorded in inside-out patches at several potentials in the range of 0 to +50 mV in the absence (○; $n = 5$) and presence of 300 nM DiBAC$_4$(3) (●; $n = 5$). The single-channel conductance was obtained from the fitting of each set of data with a linear line. E, the relationships between the relative P_o and the membrane potential were obtained from single-channel rBK$\alpha\beta$1 currents in inside-out patches. The relative P_o was determined at several potentials in the range of +30 to +130 mV in the absence (○; $n = 5$) and presence of 300 nM DiBAC$_4$(3) (●; $n = 5$). The data were fitted by a Boltzmann relationship.

Ca^{2+} concentrations, the channel activity was also measured in inside-out patch configuration at pCa values of 6.0 and 9.0. The application of 300 nM $DiBAC_4(3)$ increased the P_o at potentials examined in pCa 6.0 solution; at −30 mV, P_o was increased from 0.042 ± 0.021 to 0.226 ± 0.113 ($n = 3$, $p < 0.05$). At pCa 9.0, the P_o also tended to be increased by 300 nM $DiBAC_4(3)$ at potentials examined (from 0.185 to 0.364 at +170 mV, $n = 2$). The enhancement of rBK$\alpha\beta$1 channel activity by $DiBAC_4(3)$ was observed in a wide range of pCa values in the bathing solution in inside-out patch configuration.

Likewise, whole-cell and single-channel currents in HEK-rBKα alone were measured under the same sets of conditions as used for HEK-rBK$\alpha\beta$1. Relative P_o in the inside-out patch configuration was normalized by P_o before the application of $DiBAC_4(3)$ (Fig. 4A). The relative P_o of rBKα channels was not markedly changed by cumulative application of $DiBAC_4(3)$ in the range of 10 nM to 3 μM, (Fig. 4, A and B). Concentration-response relationships between the relative P_o of rBKα channels and $DiBAC_4(3)$ are summarized in Fig. 4C. Application of 300 nM $DiBAC_4(3)$ did not affect significantly the outward currents in HEK-rBKα under the whole-cell voltage-clamp configuration (Fig. 4D). The addition of 1 μM penitrem A abolished the outward currents. The relationships between current density and test potentials are shown in Fig. 4E. The peak outward current densities at +60 mV were 152.8 ± 70.2, 145.5 ± 67.2 ($p > 0.05$ versus the control), and 6.8 ± 3.3 pA/pF [$p < 0.01$ versus the control and in the presence of $DiBAC_4(3)$] in the absence or presence of 300 nM $DiBAC_4(3)$ and after the addition of penitrem A, respectively ($n = 3$ for each).

Selectivity of $DiBAC_4(3)$ for Subtypes of BK Channel β Subunits. In the next series of experiments, the selectivity of $DiBAC_4(3)$-induced enhancement for subtypes of BKβ was examined using HEK-rBK$\alpha\beta$2 and HEK-rBK$\alpha\beta$4 in addition to HEK-rBK$\alpha\beta$1. Whole-cell currents were measured in HEK-rBK$\alpha\beta$2 in the standard solution with the pipette solution of pCa 6.0. Under these conditions, rapidly inactivating outward currents, which have been reported as BK$\alpha\beta$2 current (Wallner et al., 1999), were detected in the voltage range from +20 to +80 mV. The outward currents, which were elicited by depolarization from a holding potential of −80 mV in 20-mV steps for 1000 ms in HEK-rBK$\alpha\beta$2, were rapidly

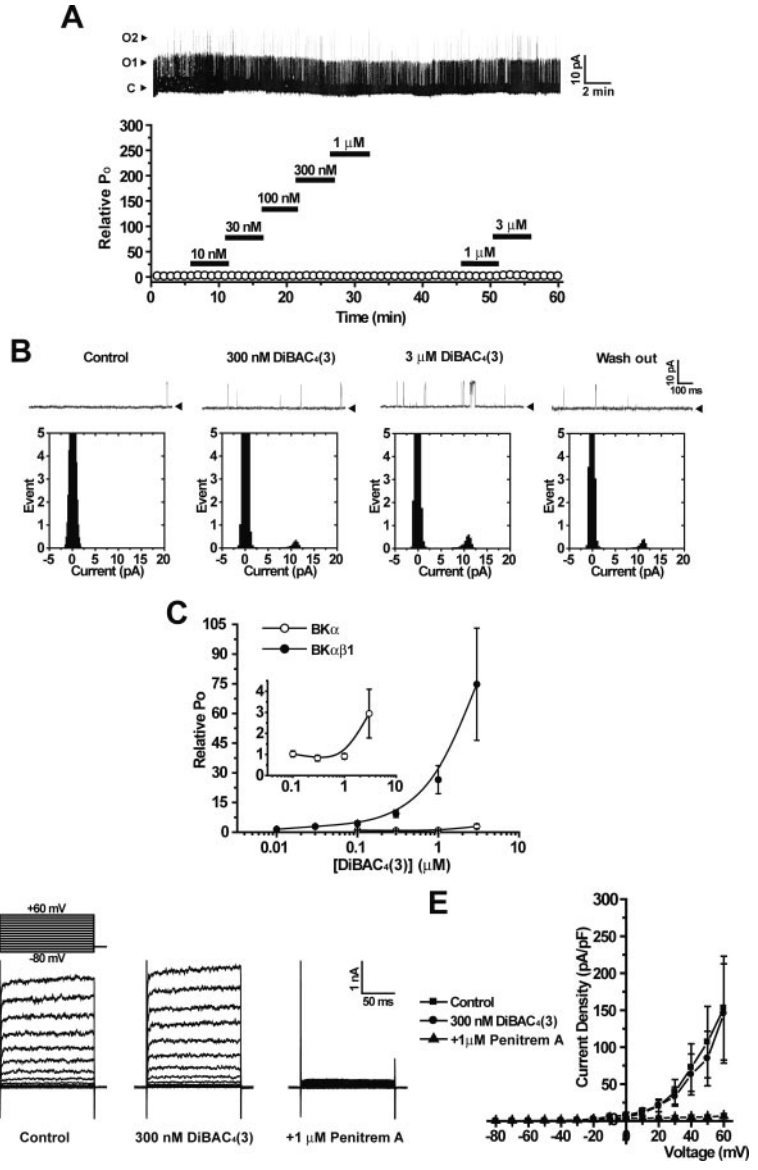

Fig. 4. Effects of $DiBAC_4(3)$ on single-channel and whole-cell rBKα currents in HEK293 cells. A, effects of $DiBAC_4(3)$ on single-channel current of rBKα alone were examined. Single-channel rBKα currents were measured under the inside-out patch configuration in symmetrical 140 mM K^+ conditions with 100 nM free Ca^{2+} in the bath and pipette solution (pCa 7.0) at a holding potential of +40 mV. $DiBAC_4(3)$ was applied cumulatively in the concentration range of 10 nM to 3 μM and then washed out. Relative P_o was normalized by P_o before the application of $DiBAC_4(3)$. C, O1, and O2 indicate closed and open state levels, respectively. Unlike in the case of rBK$\alpha\beta$1 channels, the relative P_o of rBKα channels (○) was not changed by cumulative application of $DiBAC_4(3)$. B, original traces and amplitude histograms in the control, in the presence of 300 nM or 3 μM $DiBAC_4(3)$, and after washout were obtained from the recording shown in A. The arrowhead indicates the closed state level of BK channels. C, concentration-response relationships of $DiBAC_4(3)$ on relative P_o of rBKα channels (○; $n = 3$) were obtained from experiments shown in A. Concentration-response relationships of $DiBAC_4(3)$ on relative P_o of rBK$\alpha\beta$1 channels (●; $n = 4$) shown in Fig. 3C were replotted for comparison. The inset shows the scaled concentration-response relationships of $DiBAC_4(3)$ on relative P_o of rBKα channels. D, whole-cell rBKα currents were measured in physiological K^+ gradient conditions (5.9 mM K^+ outside and 140 mM K^+ inside) with 300 nM free Ca^{2+} in the pipette solution (pCa 6.5). Each cell was depolarized from a holding potential of −60 mV to +60 mV in 10-mV steps for 150 ms at 15-s intervals. Whole-cell rBKα currents were measured in the control, in the presence of 300 nM $DiBAC_4(3)$, and after the addition of 1 μM penitrem A. E, the current-voltage relationships were obtained in the control (■; $n = 3$), in the presence of 300 nM $DiBAC_4(3)$ (●; $n = 3$), and after the addition of 1 μM penitrem A (▲; $n = 3$).

inactivated at potentials positive to +20 mV (Fig. 5A). Unlike in HEK-rBKα and HEK-rBK$\alpha\beta$1 cells, the inactivating outward currents in HEK-rBK$\alpha\beta$2 were not affected and were significantly blocked by the application of 3 μM DiBAC$_4$(3). Further addition of 1 μM penitrem A completely blocked the currents (Fig. 5A). The relationships between current density and test potentials are shown in Fig. 5B. The peak outward current densities at +80 mV in the control, in the presence of 3 μM DiBAC$_4$(3) and after the addition of penitrem A, were 199.1 ± 35.6, 135.0 ± 26.0 ($p > 0.05$ versus the control), and 7.8 ± 2.3 pA/pF [$p < 0.01$ versus the control and in the presence of DiBAC$_4$(3)], respectively ($n = 3$ for each). The relative amplitudes at +80 mV were 0.878 ± 0.090 ($p > 0.05$) and 0.627 ± 0.069 ($p < 0.01$) in 1 and 3 μM DiBAC$_4$(3), respectively ($n = 5$ for each) (Fig. 5C).

The whole-cell currents in HEK-rBK$\alpha\beta$4 were also measured under the same conditions, except for pCa in the pipette solution (pCa 6.5). The outward currents in HEK-rBK$\alpha\beta$4 cells were markedly enhanced at potentials positive to −20 mV by the application of 300 nM DiBAC$_4$(3) and then were completely blocked by the addition of 1 μM penitrem A (Fig. 6A). The relationships between current density and test potentials are shown in Fig. 6B. The peak outward current densities at +60 mV in the control, in the presence of DiBAC$_4$(3), and after the addition of penitrem A were 127.6 ± 17.9 ($n = 6$), 230.5 ± 36.1 ($n = 6$; $p < 0.01$ versus the control), and 9.4 ± 2.3 pA/pF [$n = 4$; $p < 0.01$ versus the control and in the presence of DiBAC$_4$(3)], respectively. The cumulative application of DiBAC$_4$(3) in the range of 10 nM to 3 μM concentration-dependently increased the outward currents at +20 mV in HEK-rBK$\alpha\beta$4 cells. The outward currents were then completely blocked by the further addition of 1 μM penitrem A (Fig. 6C). The concentration-response relationships for DiBAC$_4$(3) in HEK-rBK$\alpha\beta$4 are summarized in Fig. 6D, together with those for HEK-rBK$\alpha\beta$1, which are shown in Fig. 2D. It is noteworthy that the enhancement of rBK$\alpha\beta$4 currents by DiBAC$_4$(3) in the concentration range of 10 nM to 3 μM was not apparently different from that of corresponding rBK$\alpha\beta$1 currents. The relative amplitude of rBK$\alpha\beta$4 current at +20 mV in the presence of 10 nM DiBAC$_4$(3) was 1.322 ± 0.096 of the control ($p < 0.05$ versus 1.0), which was not significantly different from that of rBK$\alpha\beta$1 (1.440 ± 0.242; $p > 0.05$ versus BK$\alpha\beta$4).

Selectivity of DiBAC$_4$(3) for Other K$^+$ Channels. In the next series of experiments, the selectivity of DiBAC$_4$(3) for other K$^+$ channels, such as small-conductance Ca^{2+}-activated K$^+$ (rSK2, mSK4) channels and voltage-gated K$^+$ (rKv1.1, rKv4.3) channels, was examined by patch-clamp techniques using HEK293 cells stably expressing one of these channel α subunits (HEK-rSK2, HEK-mSK4, HEK-rKv1.1, and HEK-rKv4.3).

Whole-cell currents in HEK-rSK2 and HEK-mSK4 elicited by a ramp pulse from −160 to +20 mV for 250 ms were measured in the standard solution by use of a pipette solution, in which Cl$^-$ was replaced by aspartate$^-$, and pCa was set at 6.0. Whole-cell currents in HEK-rSK2 were slightly reduced by application of 10 μM DiBAC$_4$(3) and were blocked by the addition of 10 nM UCL 1684, a selective SK1–3 channel blocker (Fig. 7A). Whole-cell currents in HEK-mSK4 were not changed by the application of 10 μM DiBAC$_4$(3) and were blocked by the addition of 1 μM clotrimazole, an SK4 channel blocker (Fig. 7B).

Whole-cell currents in HEK-rKv1.1 and HEK-rKv4.3, elicited by depolarization from holding potential of −80 to +20 mV for 1000 ms, were measured with the pipette solution of pCa 8.0. Whole-cell currents in HEK-rKv1.1 were not changed by 10 μM DiBAC$_4$(3) and were blocked by the addition of 100 nM margatoxin, a Kv1.x-channel blocker (Fig. 7C). Whole-cell currents in HEK-rKv4.3 cells were also not affected by 10 μM DiBAC$_4$(3) (Fig. 7D).

Figure 7E summarizes data on the effects of 10 μM DiBAC$_4$(3) on these channel currents. The K$^+$ current am-

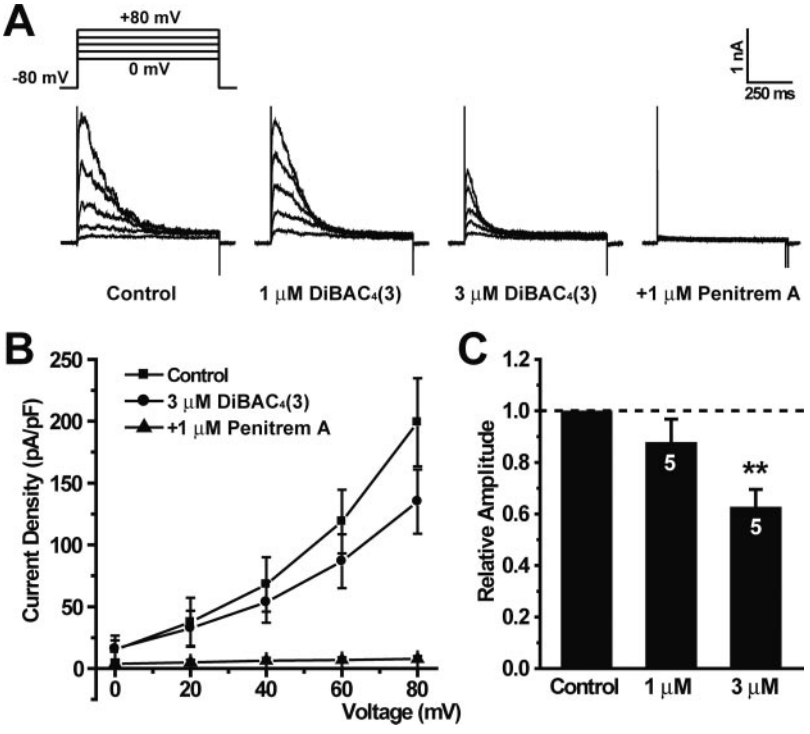

Fig. 5. Effects of DiBAC$_4$(3) on whole-cell rBK$\alpha\beta$2 currents in HEK293 cells. Whole-cell rBK$\alpha\beta$2 currents were measured in physiological K$^+$ gradient conditions (5.9 mM K$^+$ outside and 140 mM K$^+$ inside) with 1 μM free Ca^{2+} in the pipette solution (pCa 6.0). A, each cell was depolarized from a holding potential of −80 mV to +80 mV in 20-mV steps for 1000 ms at 15-s intervals. Whole-cell rBK$\alpha\beta$2 currents were measured in the control, in the presence of 1 and 3 μM DiBAC$_4$(3), and after the addition of 1 μM penitrem A. B, the current-voltage relationships were obtained in the control (■; $n = 3$), in the presence of 3 μM DiBAC$_4$(3) (●; $n = 3$), and after the further addition of 1 μM penitrem A (▲; $n = 3$). C, Concentration-response relationships of DiBAC$_4$(3) on whole-cell rBK$\alpha\beta$2 currents were obtained. Each cell was depolarized from a holding potential of −80 mV to +80 mV for 1000 ms at 15-s intervals. The relative amplitude was obtained by normalizing the peak outward current by that before the application of DiBAC$_4$(3). The numbers of individual experiments performed are indicated in columns. **, $p < 0.01$ versus 1.0.

plitude in HEK-rSK2 and HEK-mSK4 was normalized by the control current at −50 mV, corresponding to the calculated reversal potential of Cl^- in each experiment. The K^+ current amplitude in HEK-rKv1.1 and that in HEK-rKv4.3 were normalized by the peak outward current in the control at +20 mV in each cell. The relative amplitudes in the presence of 10 μM $DiBAC_4(3)$ versus the control were 0.754 ± 0.052 ($p < 0.05$ versus 1.0) in HEK-rSK2, 1.051 ± 0.057 ($p > 0.05$) in HEK-mSK4, 1.010 ± 0.013 ($p > 0.05$) in HEK-rKv1.1, and 0.942 ± 0.055 ($p > 0.05$) in HEK-rKv4.3, respectively ($n = 4$ for each). These results strongly suggest that $DiBAC_4(3)$ is selective for BK channels, more than the other Ca^{2+}-activated or voltage-gated K^+ channels examined here.

Structure-Potency Relationship of $DiBAC_4(3)$ and Related Oxonol Compounds as BK Channel Openers. Based on a distinctive structure of $DiBAC_4(3)$, in which two 1,3-dialkylbarbituric acids were connected and conjugated by the oligomethine, we performed structure-activity relationships using 16 compounds of $DiBAC_4(3)$ and its analogs to determine the structure-potency relationship for BK channel activation and the essential moiety in the molecular structure of $DiBAC_4(3)$. The generic names and structures of $DiBAC_4(3)$ and its analogs used here are listed in Fig. 8A. Figure 8B shows the effects of 100 nM and 1 μM $DiSBAC_2(5)$ (left) and of 1 and 10 μM $DiSBAC_2(1)$ (right) on the amplitude of whole-cell outward current elicited by depolarization from −60 to +20 mV in HEK-rBK$\alpha\beta$1. Application of 1 μM $DiSBAC_2(5)$ or 10 μM $DiSBAC_2(1)$ obviously or slightly enhanced rBK$\alpha\beta$1 currents, respectively. Similar experiments were performed using the listed compounds to determine their potencies (data not shown). The peak amplitude of BK currents in the presence of the test compound was normalized by that before the application and is shown in Fig. 8C.

Whole-cell currents in HEK-rBK$\alpha\beta$1 cells were enhanced by approximately 2-fold by the application of 100 nM $DiSBAC_4(3)$ (2.415 ± 0.390, $n = 5$). This was the same degree of enhancement as achieved by 100 nM $DiBAC_4(3)$ (2.262 ± 0.096, $n = 7$; $p > 0.05$ between them), indicating that the replacement of the carbon-oxygen (C=O) bonds in DiBAC to carbon-sulfur (C=S) bonds in DiSBAC did not affect BK channel activation ability. Moreover, the currents were also enhanced by approximately 2-fold by 100 nM $DiSBAC_2(3)$ [2.044 ± 0.32, $n = 4$; $p > 0.05$ versus $DiBAC_4(3)$ and $DiSBAC_4(3)$]. In contrast, the effect of the extension of alkyl side chains in the 1- to 3-positions was not clear, because extension of the side chain makes the oxonol compounds hydrophilic. For example, $DiSBAC_{10}(3)$ was too hydrophobic to dissolve in water even with methyl acetate, so the effects of $DiSBAC_{10}(3)$ on BK channels could not be determined exactly (data not shown). $DiSBAC_0(5)$ at concentrations of 1 and 10 μM did not show potency (1.017 ± 0.011, $n = 5$; $p > 0.05$ versus 1.0 and 1.003 ± 0.006, $n = 5$; $p > 0.05$ versus 1.0, respectively). In addition, under the inside-out patch configurations, $DiSBAC_0(5)$ did not increase the number of channels times P_o at 1 μM and significantly inhibited it at 10 μM. The relative number of channels times P_o values was 1.180 ±

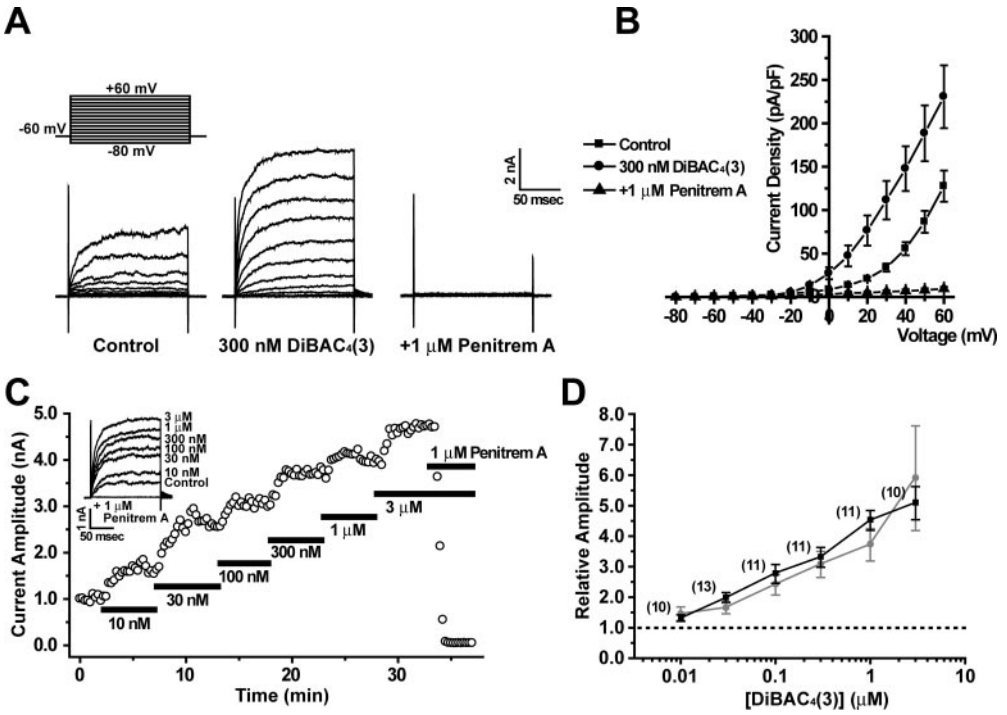

Fig. 6. Effects of $DiBAC_4(3)$ on whole-cell rBK$\alpha\beta$4 currents in HEK293 cells. Whole-cell rBK$\alpha\beta$4 currents were measured in physiological K^+ gradient conditions (5.9 mM K^+ outside and 140 mM K^+ inside) with 300 nM free Ca^{2+} in the pipette solution (pCa 6.5). A, each cell was depolarized from a holding potential of −60 mV to +60 mV in 10-mV steps for 150 ms at 15-s intervals. Whole-cell rBK$\alpha\beta$4 currents were measured in the control, in the presence of 300 nM $DiBAC_4(3)$, and after the addition of 1 μM penitrem A. B, the current-voltage relationships were obtained in the control (■; $n = 6$), in the presence of 300 nM $DiBAC_4(3)$ (●; $n = 6$), and after the addition of 1 μM penitrem A (▲; $n = 4$). C, $DiBAC_4(3)$ was applied cumulatively in the concentration range of 10 nM to 3 μM, and then 1 μM penitrem A was further added. Each cell was depolarized from a holding potential of −60 mV to +20 mV (○) for 150 ms at 15-s intervals. The peak outward current amplitude was plotted against time. Original current traces at different concentrations are superimposed and shown in the inset. D, concentration-response relationships of $DiBAC_4(3)$ on whole-cell rBK$\alpha\beta$4 currents (■) were obtained from experiments typically shown in C. The relative amplitudes were obtained by normalizing the peak outward current by that before the application of $DiBAC_4(3)$. Concentration-response relationships of $DiBAC_4(3)$ on whole-cell rBK$\alpha\beta$1 currents (●) shown in Fig. 2D were replotted for comparison. The numbers of individual experiments performed are indicated in parentheses.

0.217 ($n = 6$; $p > 0.05$ versus 1.0) and 0.422 ± 0.146 ($n = 4$; $p < 0.05$ versus 1.0) in the presence of 1 and 10 μM DiSBAC$_0$(5), respectively. Therefore, the lack of the side chains may markedly decrease efficacy. From these results, it can be suggested that the alkyl side chains in the 1- to 3-positions are essential for the BK channel-opening property but that the length between C2 (ethyl) and C4 (butyl) seems to be not very critical to efficacy.

To reveal the importance of the two barbituric rings, which are conjugated by an oligomethine chain in DiBAC$_4$(3), we examined the effects of barbiturates, clinically used as hypnotics (hexobarbital and barbital), hydantoin anticonvulsants (phenytoin), and barbituric/thiobarbituric acids (BA, DMBA, and DETBA) on whole-cell currents in HEK-rBK$\alpha\beta$1. The results revealed no ability to activate the BK channel when 10 μM hexobarbital, barbital, or phenytoin was applied (data not shown). Application of 10 μM BA, DMBA, or DETBA likewise did not affect BK currents in HEK-rBK$\alpha\beta$1 (Fig. 8C). The relative amplitudes were 0.996 ± 0.039 ($n = 5$; $p > 0.05$ versus 1.0), 0.938 ± 0.028 ($n = 4$; $p > 0.05$ versus 1.0), and 1.125 ± 0.096 ($n = 4$; $p > 0.05$ versus 1.0) in the presence of 10 μM BA, DMBA, and DETBA, respectively. These results strongly suggest that the two barbituric rings conjugated by an oligomethine chain are essential for the BK channel-opening efficacy of DiBAC$_4$(3).

To determine whether the length of the oligomethine chain is an important factor in determining potency, the effects of DiBAC$_4$(3) and DiSBAC$_2$(3) were compared with those of corresponding compounds having longer pentamethine chains, DiBAC$_4$(5) and DiSBAC$_2$(5), respectively. Moreover, the effects of DiSBAC$_2$(1), in which the chain is just methine, were also examined. It is interesting that the relative amplitudes were 1.257 ± 0.025 ($n = 5$; $p < 0.01$ versus 1.0) and 1.293 ± 0.033 ($n = 4$; $p < 0.01$ versus 1.0) in the presence of 100 nM DiBAC$_4$(5) and DiSBAC$_2$(5), respectively, and 1.918 ± 0.287 ($n = 5$; $p < 0.05$ versus 1.0) and 2.107 ± 0.053 ($n = 4$; $p < 0.01$ versus 1.0) at 1 μM DiBAC$_4$(5) and DiSBAC$_2$(5), respectively. The potency of DiSBAC$_2$(1) was not detected at 1 μM (1.044 ± 0.050, $n = 4$; $p > 0.05$ versus 1.0) but was at 10 μM (1.252 ± 0.063, $n = 4$; $p < 0.05$ versus 1.0)

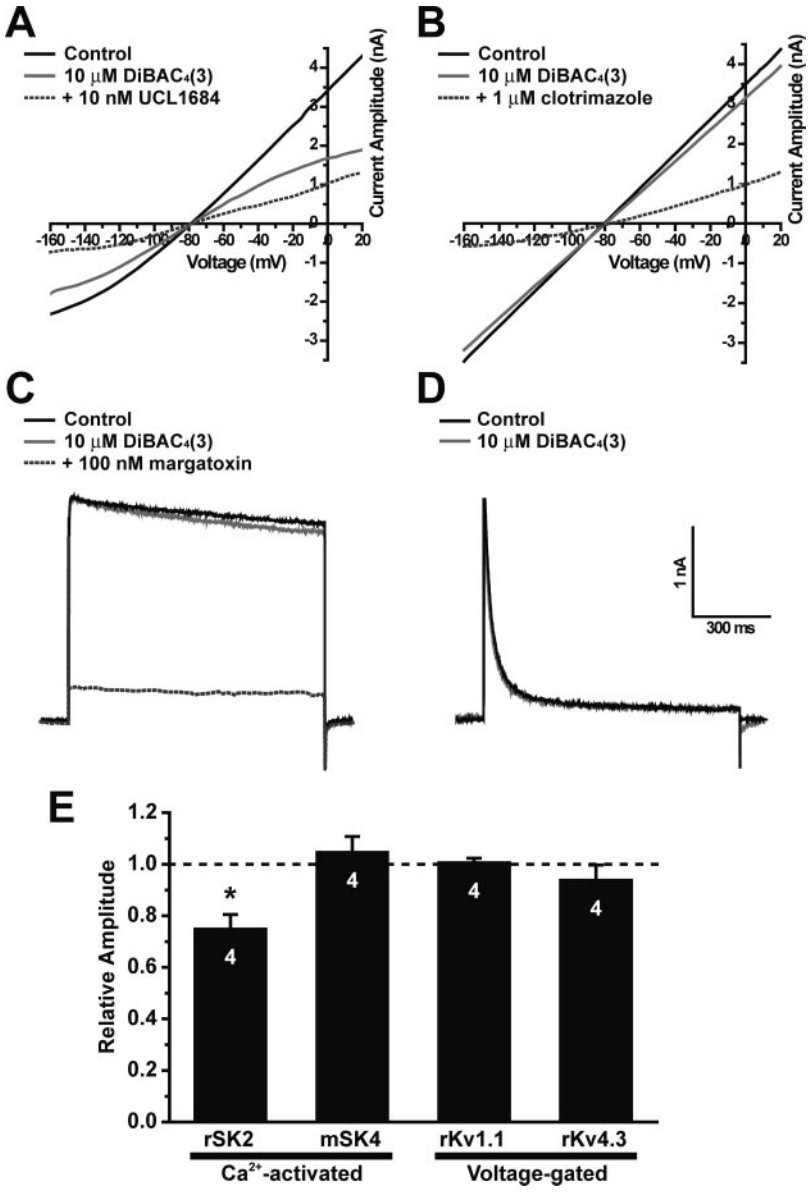

Fig. 7. Effects of DiBAC$_4$(3) on other K^+ currents in HEK293 cells. Whole-cell K^+ currents were measured in physiological K^+ gradient conditions (5.9 mM K^+ outside and 140 mM K^+ inside). A and B, effects of 10 μM DiBAC$_4$(3) on type 2 small-conductance Ca^{2+}-activated K^+ channel (rSK2) (A) and type 4 (mSK4) (B) were examined. Each HEK293 cell stably expressing rSK2 or mSK4 channels was held at −90 mV and depolarized by a ramp pulse from −160 mV to +20 mV for 250 ms. The pipette solution contained 1 μM free Ca^{2+} (pCa 6.0) and aspartate$^-$, which was replaced with Cl^-. SK2 and SK4 currents were identified as the currents susceptible to 10 nM UCL 1684 (A) or 1 μM clotrimazole (B), respectively. C and D, effects of 10 μM DiBAC$_4$(3) on voltage-gated K^+ channel currents rKv1.1 (C) and rKv4.3 (D). Each cell stably expressing voltage-gated K^+ (rKv1.1, rKv4.3) channels was depolarized from a holding potential of −80 mV to +20 mV for 1000 ms. Whole-cell rKv1.1 currents were identified as the currents suppressed by 100 nM margatoxin (C). Whole-cell rKv4.3 current was identified as the rapidly inactivating current (D). E, summarized data were obtained from experiments shown in A through D. The relative amplitudes were obtained by normalizing the outward current at −50 mV corresponding to the Cl^- reversal potential in rSK2 and mSK4 channels or the peak outward current at +20 mV in rKv1.1 and rKv4.3 channels by that before the application of 10 μM DiBAC$_4$(3). The numbers of individual experiments performed are indicated in columns. *, $p <$ 0.05 versus 1.0.

(Fig. 8C). Thus, "trimethine" is the best length of the oligomethine chain. These results suggest that the length of conjugating oligomethine is a key factor in determining the potency of bis-barbituric acid oxonol compounds as BK channel openers.

To reveal the number of oxo-moieties and the locations in the molecule that would endow potency, the effects of Oxonol 595, Oxonol V, and Oxonol VI were examined. Oxonol 595 has a structure similar to that of $DiBAC_4(3)$, whereas oxo-moieties do not exist in the 4-position of pyrimidine. Oxonol V and Oxonol VI have a 5-isoxazolone structure. It is surprising that Oxonol 595 did not show potency at all (1.002 ± 0.025, $n = 4$; $p > 0.05$ versus 1.0 and 1.071 ± 0.078, $n = 5$; $p > 0.05$ in the presence of 1 and 10 μM Oxonol 595, respectively). In contrast, both Oxonol V and Oxonol VI act as BK channel openers, but the potency of Oxonol V was approximately 10-fold higher than that of Oxonol VI (Fig. 8D). Based on the acidic pK_a, oxonol must almost completely form an oxoanion at pH 7.4 (Table 1). It was mysterious, however, that Oxonol 595 did not show any potency as a BK channel opener even at 10 μM.

Stereochemical Analyses of Essential Moiety in the Molecular Structure of $DiBAC_4(3)$ for BK Channel Activation. To elucidate two questions—1) why was Oxonol 595 not potent, and 2) what is the most effective length of oligomethine between oxo- and oxoanion-moieties in a molecule—we performed stereochemical analyses by calculating the most stable stereochemical structures of oxonol compounds using the DFT methods in Spartan (see *Materials and Methods*).

Figure 9A shows top and side views of the most stable stereochemical structures of the 10 oxonol compounds examined in this study. Table 1 shows the interatomic distance between oxo- and oxoanion-moieties in each side of the oligomethine chain in a molecule and the potency as a relative enhancement of whole-cell current in HEK-rBK$\alpha\beta$1. It is notable that the negatively charged oxygen atoms indicated by arrows in Fig. 9A and the oligomethine chain are the most stable in a single plane, based on the side views of these molecules. The most striking finding here is that the oxo- and oxoanion-moieties in Oxonol 595 are located on different sides of the conjugated oligomethine chain (sky blue and pink arrows in Fig. 9A). Judging from the potency and the distance between oxo- and oxoanion-moieties in Oxonol V and Oxonol VI, it may be essential for potency that at least one set of oxo- and oxoanion-moieties, which are conjugated by oligomethine, should be on one side of the methine chain in

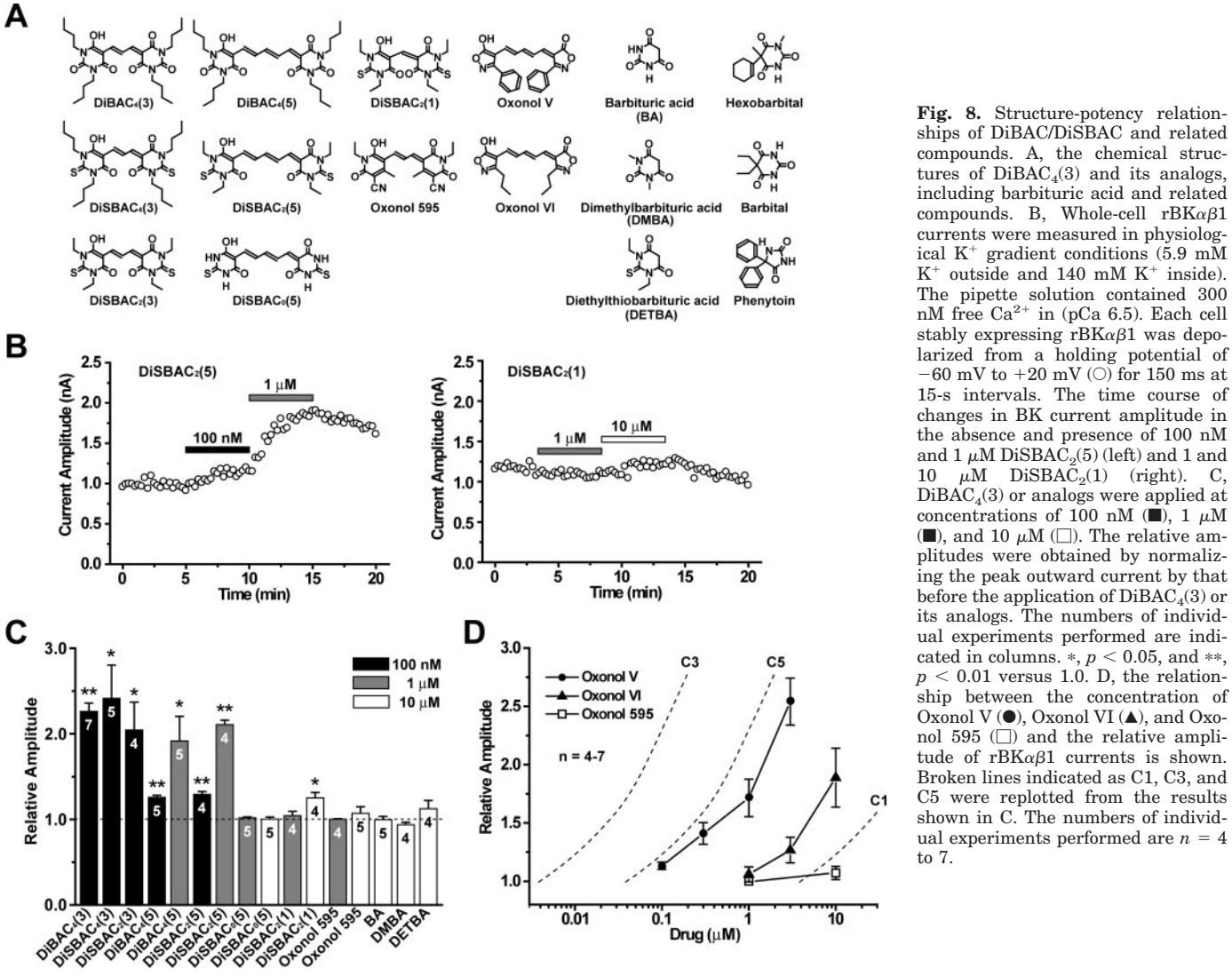

Fig. 8. Structure-potency relationships of DiBAC/DiSBAC and related compounds. A, the chemical structures of $DiBAC_4(3)$ and its analogs, including barbituric acid and related compounds. B, Whole-cell rBK$\alpha\beta$1 currents were measured in physiological K^+ gradient conditions (5.9 mM K^+ outside and 140 mM K^+ inside). The pipette solution contained 300 nM free Ca^{2+} in (pCa 6.5). Each cell stably expressing rBK$\alpha\beta$1 was depolarized from a holding potential of −60 mV to +20 mV (○) for 150 ms at 15-s intervals. The time course of changes in BK current amplitude in the absence and presence of 100 nM and 1 μM $DiSBAC_2(5)$ (left) and 1 and 10 μM $DiSBAC_2(1)$ (right). C, $DiBAC_4(3)$ or analogs were applied at concentrations of 100 nM (■), 1 μM (■), and 10 μM (□). The relative amplitudes were obtained by normalizing the peak outward current by that before the application of $DiBAC_4(3)$ or its analogs. The numbers of individual experiments performed are indicated in columns. *, $p < 0.05$, and **, $p < 0.01$ versus 1.0. D, the relationship between the concentration of Oxonol V (●), Oxonol VI (▲), and Oxonol 595 (□) and the relative amplitude of rBK$\alpha\beta$1 currents is shown. Broken lines indicated as C1, C3, and C5 were replotted from the results shown in C. The numbers of individual experiments performed are $n = 4$ to 7.

the stereochemical structure (Fig. 9B). The calculated interatomic oxygen-oxygen distances on each side of the oligomethine chain in the DiBAC/DiSBAC compounds were 4.1 (short) and 6.7 Å (long) in trimethine oxonols [DiBAC$_4$(3), DiSBAC$_4$(3), and DiSBAC$_2$(3)], 6.7 (short) and 9.1 Å (long) in pentamethine oxonols [DiBAC$_4$(5) and DiSBAC$_2$(5)], and 2.7 (short) and 4.7 Å (long) in methine oxonol [DiSBAC$_2$(1)] (Table 1).

Discussion

The Selectivity of DiBAC$_4$(3) for Regulatory β Subunit and Speculation on the Binding Site on BK Channel. In this study, we clearly demonstrated that DiBAC$_4$(3) selectively activates the BK channel only when the regulatory rBKβ1 or rBKβ4, but not rBKβ2, is coexpressed with rBKα in HEK293 cells. The finding that DiBAC$_4$(3) markedly enhanced BK current in mUBSMCs, in which BK channels are composed of BKα and BKβ1 (Petkov et al., 2001), indicates that DiBAC$_4$(3) can work as a potent BKαβ1 channel opener in native cells. Although the BKβ is a potential target of drug development, very limited information is available about chemicals that selectively act on BKβ as BK channel openers. Most BK channel openers that have been developed act on the α subunit (Imaizumi et al., 2002; Nardi et al., 2003), and only a few compounds have been reported as β-subunit-selective BK channel openers: β-estradiol (Valverde et al., 1999), tamoxifen (Dick et al., 2001), and dehydrosoyasaponin-I (DHS-I) (McManus et al., 1995; Giangiacomo et al., 1998).

DHS-I activates the BK channel only in the presence of the β1 subunit by intracellular application. This is due to the low membrane permeability and the negative charge in the structure at physiological pH. DHS-I also activates the BK channel in the presence of human BKβ2 without the inactivation domain by intracellular application (Wallner et al., 1999). Although the effects of β-estradiol and tamoxifen on BKβ2 have not been reported, they are effective on both BKβ1 and BKβ4. It is therefore noteworthy that DiBAC$_4$(3) enhanced the currents through rBKαβ1 and rBKαβ4 but not through rBKαβ2. DiBAC$_4$(3) did not modify the single-channel conductance but enhanced markedly the voltage sensitivity in the rBKαβ1 channel. These properties of DiBAC$_4$(3)-induced activation of the rBKαβ1 channel seemed to be shared with the rBKαβ4 channel (data not shown). Moreover, the concentration-response relationship for DiBAC$_4$(3)-induced enhancement of the rBKαβ4 current was comparable with that of the rBKαβ1 current. These results may suggest that the DiBAC$_4$(3) binding site is in the amino acid sequences that are common between BKβ1 and BKβ4 but not with BKβ2. Based on the sequence analysis, rBKβ1 shares only 23% sequence homology with rBKβ4 but 41% with rBKβ2. Detection of the exact location of the DiBAC$_4$(3) binding site in BKβ1 and BKβ4 will provide new insight into the functional coupling of BKβ with BKα.

Selectivity of DiBAC$_4$(3) for BK Channel versus Other Channels. Small-conductance Ca^{2+}-activated K^+ (rSK2, mSK4) channels and voltage-gated K^+ (rKv1.1, rKv4.3) channels were not affected by 10 μM DiBAC$_4$(3). Because DiBAC$_4$(3) has been used for the screening of K_{ATP} channel modulators at a concentration of 5 μM (Whiteaker et al., 2001), we presume that the K_{ATP} channel is also unaffected by DiBAC$_4$(3). In our preliminary study, 1 μM DiBAC$_4$(3) did not affect the voltage-dependent Ca^{2+} channel in mUBSMCs (T. Morimoto, unpublished observation). However, it has been reported that DiBAC$_4$(5) inhibits a volume-sensitive Cl^- channel (Arreola et al., 1995) and anion exchangers (AE) such as the AE1 Cl^-/HCO_3^- exchanger in red blood cells and AE2 in HL-60 cells (Alper et al., 1998). In our previous study, in which we assayed pimaric acids and related compounds as BK channel openers, we measured successfully membrane potential changes in HEK-rBKαβ1 by using DiBAC$_4$(3) at a concentration of 50 nM (Yamada et al., 2001; Imaizumi et al., 2002) but in the present study, we did not detect any changes at 1 μM (data not shown). Based on these results, DiBAC$_4$(3) as a voltage indicator should be used at low concentrations (<100 nM) to avoid artifacts that are a result of the direct action on ion channels. It is also noteworthy that DiBAC$_4$(3) binds to cytosolic proteins, presumably in a nonspecific fashion, and this elongates markedly the fluorescence lifetime after excitation (González et al., 1999). This means that DiBAC/DiSBAC dyes can bind many types of ion channel proteins, regardless of whether or not they express specific effects. Considering the possibility that DiBAC$_4$(3) may also bind to peptide BK channel block-

TABLE 1

The interatomic distance between two oxygen atoms and the potency of oxonol compounds as BK channel openers

The pK_a value and interatomic distance between two oxygen atoms on one side of the oligomethine in DiBAC$_4$(3) and its analogs. The potency to enhance the whole-cell BK channel currents in HEK293 cells in which rBKαβ1 was stable is expressed.

Generic Name	pK_a	Oxygen-Oxygen Distance		Potency on Whole-Cell Current in HEK-rBKαβ1		
		Short	Long	100 nM	1 μM	10 μM
		Å				
DiBAC$_4$(3)	2.17 ± 0.60	3.81	6.61	2.26 ± 0.10**	3.72 ± 0.53**	N.D.
DiSBAC$_4$(3)	1.72 ± 0.60	4.18	6.71	2.42 ± 0.39*	N.D.	N.D.
DiSBAC$_2$(3)	1.72 ± 0.60	4.18	6.70	2.04 ± 0.32*	N.D.	N.D.
DiBAC$_4$(5)	3.96 ± 0.60	6.74	9.07	1.26 ± 0.03**	1.92 ± 0.29*	N.D.
DiSBAC$_2$(5)	3.53 ± 0.60	6.73	9.08	1.29 ± 0.03**	2.11 ± 0.05**	N.D.
DiSBAC$_0$(5)	3.50 ± 0.20	6.80	9.22	N.D.	1.02 ± 0.01	1.00 ± 0.01
DiSBAC$_2$(1)	2.42 ± 0.60	2.65	4.69	N.D.	1.04 ± 0.05	1.25 ± 0.06*
Oxonol 595	N.D.			N.D.	1.00 ± 0.03	1.07 ± 0.08
Oxonol V	5.18 ± 0.20		9.67	1.13 ± 0.03*	1.72 ± 0.16**	N.D.
Oxonol VI	5.52 ± 0.20		9.53	N.D.	1.06 ± 0.06	1.89 ± 0.25*

N.D., not determined.
* $p < 0.05$.
** $p < 0.01$ vs. 1.0 ($n = 4$–7).

ers, iberiotoxin and charybdotoxin, we prefer to use small molecules such as penitrem A to block BK channels.

Essential Moiety in the Molecular Structure of DiBAC$_4$(3) for BK Channel Activation. Barbiturate derivatives are rather old hypnotics and have been used at relatively high plasma concentrations. Because the DiBAC$_4$(3) molecule includes two barbituric acids, we at first considered the possibility that barbituric acid and its derivatives may work as BK channel openers. The present results, however, showed clearly that this is not the case; none of the barbituric acid-related compounds used in this study had sufficient potency. In addition, DiSBAC$_4$(3) possessed high potency, which was comparable with that of DiBAC$_4$(3). Therefore, the chemical structure of two barbituric/thiobarbituric acids conjugated with a certain length of oligomethine chain seems to be essential for DiBAC/DiSBAC compounds to have a BK channel-opening property. The length of the oligomethine chain modified substantially the potency of the molecule as a BK channel opener. The potency of DiBAC$_4$(3) was reduced to 1/10 in pentamethine oxonols [DiBAC$_4$(5) and DiSBAC$_2$(5)], and to 1/1000 in methine oxonol [DiSBAC$_2$(1)], indicating the order of potency was methine (C1) $\ll$ pentamethine (C5) $<$ trimethine (C3). The length of the alkyl chain in 1,3-positions of barbituric/thiobarbituric acid also affected potency, because the potency of DiSBAC$_2$(3) (1,3-diethyl) was comparable with that of DiSBAC$_4$(3) (1,3-dibuthyl), whereas the lack of a side chain in the 1,3-positions [DiSBAC$_0$(5)] abolished the potency.

The most important finding to elucidate the fundamental moiety as a BK channel opener in DiBAC/DiSBAC compounds was that Oxonol 595 did not show potency. Based on this finding, we considered that two sets of oxo- and oxoan-

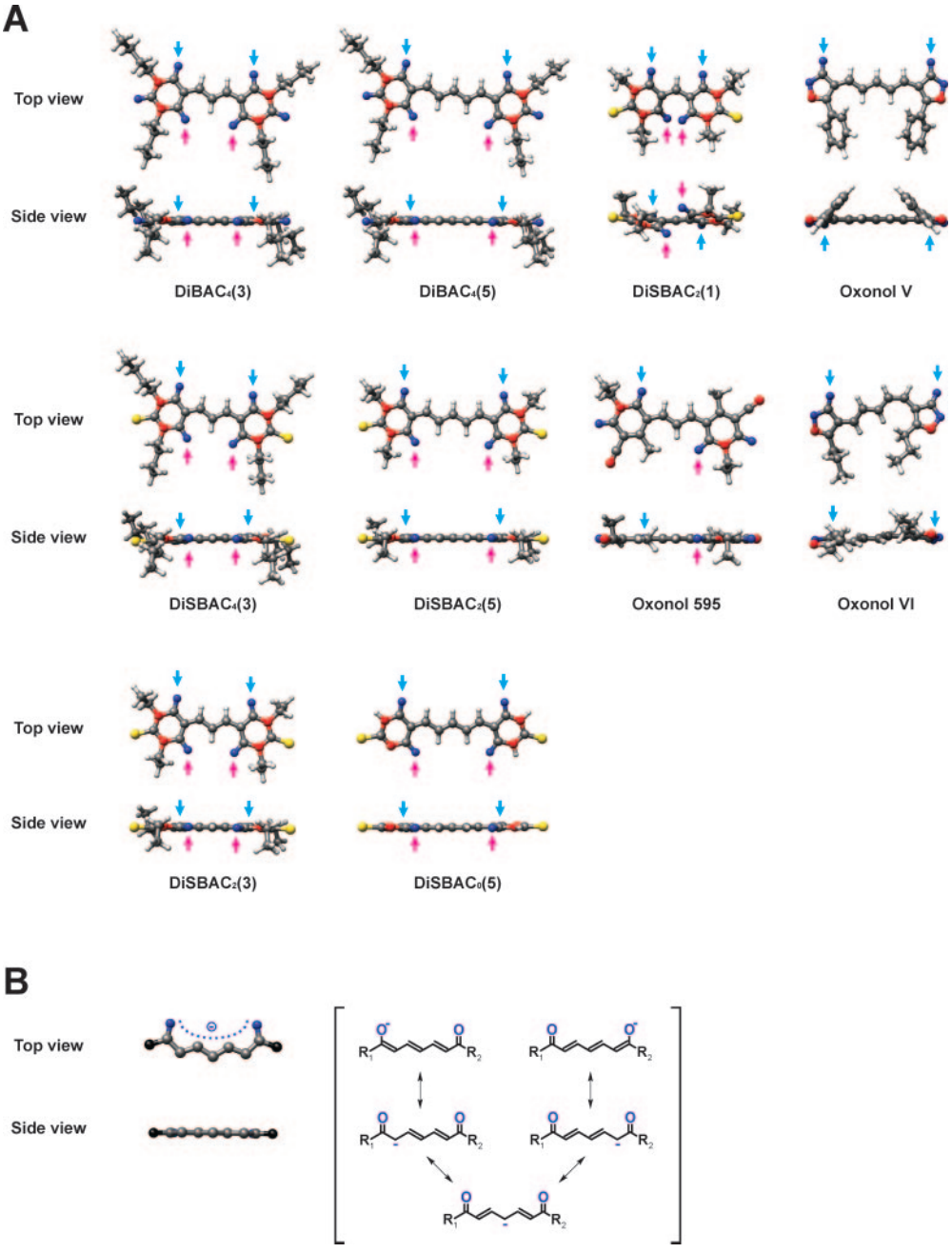

Fig. 9. The most stable stereochemical structures of oxonol compounds. The most stable stereochemical structures of oxonol compounds were calculated by using the DFT methods in Spartan software. Top and side views by University of California at San Francisco Chimera software are shown. Hydrogen, carbon, nitrogen, oxygen, and sulfur atoms in oxonol compounds are shown by white, gray, red, blue, and yellow, respectively. A, two sets of oxo- and oxoanion-moieties on each side of oligomethine are indicated by sky blue and pink arrows, respectively. The distances between oxygen atoms indicated by the sky blue and pink arrows are long and short, respectively. The oxo- and oxoanion-moieties in Oxonol V and Oxonol VI were located on the same side of the oligomethine, and those in Oxonol 595 were separated one by one on either side. B, the minimum requirement of stereochemical structure for a BK channel opener.

ion-moieties at the 4,6-positions in two barbituric acid rings are essential for potency. To confirm this assumption, we examined the effects of Oxonol V and Oxonol VI, which we supposed would be ineffective. Unexpectedly, however, they had potency. These results indicate that one set of oxo- and oxoanion-moieties that are each conjugated with an oligomethine are enough for potency as a minimum requirement. The stereochemical optimization of all the compounds used in this study, including Oxonol 595 and Oxonol V/VI, by the DFT methods (see *Materials and Methods*), revealed the mechanism underlying these unexpected results. The molecular images in the most stable stereochemical structures of these compounds indicate that the oxo- and oxoanion-moieties in Oxonol 595 are located on each side of the oligomethine, whereas those in Oxonol V/VI were on the same side, as indicated by sky blue and pink arrows in Fig. 9A. Moreover, the two barbituric/thiobarbituric acid rings and the connecting oligomethine in DiBAC/DiSBAC compounds must be in the same plane (side views in Fig. 9A). This is also the case in Oxonol V, in which the two rings are 5-isoxazolone. This may be essential for the effective electron transfer coupling between negatively charged plane oxo-groups and the connecting oligomethine chain. The molecular image of DiSBAC$_2$(1), which did not show potency, includes a twist between two thiobarbituric acid rings. Oxonol VI, which showed substantially lower potency than Oxonol V, also has a slight twist in the oligomethine in the most stable stereochemical structure (Fig. 9A).

The stereochemical analyses also allow us to calculate the interatomic distance between two oxygen atoms in the two sets of oxo- and oxoanion-moieties on each side of the oligomethine in DiBAC$_4$(3) as approximately 4 and 7 Å, respectively. In DiBAC/DiSBAC compounds, the two oxygen atoms in oxo- and oxoanion-moieties at a short distance (4 Å), which were conjugated by trimethine, would give the highest potency, presumably by the most effectively conjugated π electron transfer.

Together, these findings suggest that the minimum requirement of a stereochemical structure for BK channel openers may be as follows: one set of oxo- and oxoanion-moieties on the same side, which are conjugated by tri- or pentamethine groups, should form an electron transfer coupling structure in a single plane, as illustrated in Fig. 9B.

Conclusion

Our finding that DiBAC$_4$(3) and related oxonol compounds are β-subunit-selective BK channel openers is extremely important; not only will these compounds serve many uses as pharmacological tools and templates for the design of β-subunit-selective BK channel openers, but they will also reveal the functional coupling mechanism between pore-forming α and regulatory β subunits. This study provides a molecular and structural basis for BK channels and contributes to the understanding of the regulatory mechanism of BK channel activity by the auxiliary β subunit.

Acknowledgments

We thank Professor Naoki Miyata and Dr. Takayoshi Suzuki for calculations of the most stable stereochemical structures by using Spartan '04 software and for their helpful advice.

References

Alper SL, Chernova MN, Williams J, Zasloff M, Law FY, and Knauf PA (1998) Differential inhibition of AE1 and AE2 anion exchangers by oxonol dyes and by novel polyaminosterol analogs of the shark antibiotic squalamine. *Biochem Cell Biol* **76:**799–806.

Arreola J, Hallows KR, and Knauf PA (1995) Volume-activated chloride channels in HL-60 cells: potent inhibition by an oxonol dye. *Am J Physiol* **269:**C1063–C1072.

Brenner R, Jegla TJ, Wickenden A, Liu Y, and Aldrich RW (2000a) Cloning and functional characterization of novel large conductance calcium-activated potassium channel beta subunits, hKCNMB3 and hKCNMB4. *J Biol Chem* **275:**6453–6461.

Brenner R, Perez GJ, Bonev AD, Eckman DM, Kosek JC, Wiler SW, Patterson AJ, Nelson MT, and Aldrich RW (2000b) Vasoregulation by the beta1 subunit of the calcium-activated potassium channel. *Nature (Lond)* **407:**870–876.

Dick GM, Rossow CF, Smirnov S, Horowitz B, and Sanders KM (2001) Tamoxifen activates smooth muscle BK channels through the regulatory β1 subunit. *J Biol Chem* **276:**34594–34599.

Elkins T, Ganetzky B, and Wu CF (1986) A *Drosophila* mutation that eliminates a calcium-dependent potassium current. *Proc Natl Acad Sci USA* **83:**8415–8419.

Fernandez-Fernandez JM, Tomas M, Vazquez E, Orio P, Latorre R, Senti M, Marrugat J, and Valverde MA (2004) Gain-of-function mutation in the KCNMB1 potassium channel subunit is associated with low prevalence of diastolic hypertension. *J Clin Investig* **113:**1032–1039.

Giangiacomo KM, Kamassah A, Harris G, and McManus OB (1998) Mechanism of maxi-K channel activation by dehydrosoyasaponin-I. *J Gen Physiol* **112:**485–501.

González JE, Oades K, Leychkis Y, Harootunian A, and Negulescu PA (1999) Cell-based assays and instrumentation for screening ion-channel targets. *Drug Discov Today* **4:**431–439.

Hatano N, Ohya S, Muraki K, Clark RB, Giles WR, and Imaizumi Y (2004) Two arginines in the cytoplasmic C-terminal domain are essential for voltage-dependent regulation of A-type K^+ current in the Kv4 channel subfamily. *J Biol Chem* **279:**5450–5459.

Imaizumi Y, Sakamoto K, Yamada A, Hotta A, Ohya S, Muraki K, Uchiyama M, and Ohwada T (2002) Molecular basis of pimarane compounds as novel activators of large-conductance Ca^{2+}-activated K^+ channel α-subunit. *Mol Pharmacol* **62:**836–846.

Jepras RI, Paul FE, Pearson SC, and Wilkinson MJ (1997) Rapid assessment of antibiotic effects on *Escherichia coli* by bis-(1,3-dibutylbarbituric acid) trimethine oxonol and flow cytometry. *Antimicrob Agents Chemother* **41:**2001–2005.

Knaus HG, Folaner K, Garcia-Calvo M, Garcia ML, Kaczorowski GJ, Smith M, and Swanson R (1994) Primary sequence and immunological characterization of β-subunit of high conductance Ca^{2+}-activated K^+ channel from smooth muscle. *J Biol Chem* **269:**17274–17278.

McManus OB, Helms LM, Pallanck L, Ganetzky B, Swanson R, and Leonard RJ (1995) Functional role of the beta subunit of high conductance calcium-activated potassium channels. *Neuron* **14:**645–650.

Meera P, Wallner M, and Toro L (2000) A neuronal β subunit (KCNMB4) makes the large conductance, voltage- and Ca^{2+}-activated K^+ channel resistant to charybdotoxin and iberiotoxin. *Proc Natl Acad Sci USA* **97:**5562–5567.

Meredith AL, Thorneloe KS, Werner ME, Nelson MT, and Aldrich RW (2004) Overactive bladder and incontinence in the absence of the BK large conductance Ca^{2+}-activated K^+ channel. *J Biol Chem* **279:**36746–36752.

Morimura K, Ohi Y, Yamamura H, Ohya S, Muraki K, and Imaizumi Y (2006) Two-step Ca^{2+} intracellular release underlies excitation-contraction coupling in mouse urinary bladder myocytes. *Am J Physiol* **290:**C388–C403.

Nardi A, Calderone V, Chericoni S, and Morelli I (2003) Natural modulators of large-conductance calcium-activated potassium channels. *Planta Med* **69:**885–892.

Ohya S, Kuwata Y, Sakamoto K, Muraki K, and Imaizumi Y (2005) Cardioprotective effects of estradiol include the activation of large-conductance Ca^{2+}-activated K^+ channels in cardiac mitochondria. *Am J Physiol* **289:**H1635–H1642.

Orio P, Rojas P, Ferreira G, and Latorre R (2002) New disguises for an old channel: MaxiK channel beta-subunits. *News Physiol Sci* **17:**156–161.

Petkov GV, Bonev AD, Heppner TJ, Brenner R, Aldrich RW, and Nelson MT (2001) Beta1-subunit of the Ca^{2+}-activated K^+ channel regulates contractile activity of mouse urinary bladder smooth muscle. *J Physiol (Lond)* **537:**443–452.

Quirk JC and Reinhart PH (2001) Identification of a novel tetramerization domain in large conductance K_{Ca} channels. *Neuron* **32:**13–23.

Rüttiger L, Sausbier M, Zimmermann U, Winter H, Braig C, Engel J, Knirsch M, Arntz C, Langer P, Hirt B, et al. (2004) Deletion of the Ca^{2+}-activated potassium (BK) alpha-subunit but not the BKβ1-subunit leads to progressive hearing loss. *Proc Natl Acad Sci USA* **101:**12922–12927.

Sakamoto K, Nonomura T, Ohya S, Muraki K, Ohwada T, and Imaizumi Y (2006) Molecular mechanisms for large conductance Ca^{2+}-activated K^+ channel activation by a novel opener, 12,14-dichlorodehydroabietic acid. *J Pharmacol Exp Ther* **316:**144–153.

Sausbier M, Arntz C, Bucurenciu I, Zhao H, Zhou XB, Sausbier U, Feil S, Kamm S, Essin K, Sailer CA, et al. (2005) Elevated blood pressure linked to primary hyperaldosteronism and impaired vasodilation in BK channel-deficient mice. *Circulation* **112:**60–68.

Sausbier M, Hu H, Arntz C, Feil S, Kamm S, Adelsberger H, Sausbier U, Sailer CA, Feil R, Hofmann F, et al. (2004) Cerebellar ataxia and Purkinje cell dysfunction caused by Ca^{2+}-activated K^+ channel deficiency. *Proc Natl Acad Sci USA* **101:**9474–9478.

Schreiber M and Salkoff L (1997) A novel calcium-sensing domain in the BK channel. *Biophys J* **73:**1355–1363.

Uebele VN, Lagrutta A, Wade T, Figueroa DJ, Liu Y, McKenna E, Austin CP, Bennett PB, and Swanson R (2000) Cloning and functional expression of two families of beta-subunits of the large conductance calcium-activated K^+ channel. *J Biol Chem* **275:**23211–23218.

Valverde MA, Rojas P, Amigo J, Cosmelli D, Orio P, Bahamonde MI, Mann GE, Vergara C, and Latorre R (1999) Acute activation of Maxi-K channels (hSlo) by estradiol binding to the beta subunit. *Science (Wash DC)* **285:**1929–1931.

Vergara C, Latorre R, Marrion NV, and Adelman JP (1998) Calcium-activated potassium channels. *Curr Opin Neurobiol* **8:**321–329.

Wallner M, Meera P, and Toro L (1996) Determinant for beta-subunit regulation in high-conductance voltage-activated and Ca^{2+}-sensitive K^+ channels: an additional transmembrane region at the N terminus. *Proc Natl Acad Sci USA* **93:**14922–14927.

Wallner M, Meera P, and Toro L (1999) Molecular basis of fast inactivation in voltage and Ca^{2+}-activated K^+ channels: a transmembrane β-subunit homolog. *Proc Natl Acad Sci USA* **96:**4137–4142.

Weiger TM, Holmqvist MH, Levitan IB, Clark FT, Sprague S, Huang WJ, Ge P, Wang C, Lawson D, Jurman ME, et al. (2000) A novel nervous system beta subunit that downregulates human large conductance calcium-dependent potassium channels. *J Neurosci* **20:**3563–3570.

Whiteaker KL, Gopalakrishnan SM, Groebe D, Shieh CC, Warrior U, Burns DJ, Coghlan MJ, Scott VE, and Gopalakrishnan M (2001) Validation of FLIPR membrane potential dye for high throughput screening of potassium channel modulators. *J Biomol Screen* **6:**305–312.

Xia XM, Ding JP, and Lingle CJ (1999) Molecular basis for the inactivation of Ca^{2+}- and voltage-dependent BK channels in adrenal chromaffin cells and rat insulinoma tumor cells. *J Neurosci* **19:**5255–5264.

Xia XM, Ding JP, Zeng XH, Duan KL, and Lingle CJ (2000) Rectification and rapid activation at low Ca^{2+} of Ca^{2+}-activated, voltage-dependent BK currents: consequences of rapid inactivation by a novel beta subunit. *J Neurosci* **20:**4890–4903.

Xie J and McCobb DP (1998) Control of alternative splicing of potassium channels by stress hormones. *Science (Wash DC)* **280:**443–446.

Yamada A, Gaja N, Ohya S, Muraki K, Narita H, Ohwada T, and Imaizumi Y (2001) Usefulness and limitation of $DiBAC_4(3)$, a voltage-sensitive fluorescent dye, for the measurement of membrane potentials regulated by recombinant large conductance Ca^{2+}-activated K^+ channels in HEK293 cells. *Jpn J Pharmacol* **86:**342–350.

Zarei MM, Zhu N, Alioua A, Eghbali M, Stefani E, and Toro L (2001) A novel MaxiK splice variant exhibits dominant-negative properties for surface expression. *J Biol Chem* **276:**16232–16239.

Zeng XH, Xia XM, and Lingle CJ (2003) Redox-sensitive extracellular gates formed by auxiliary beta subunits of calcium-activated potassium channels. *Nat Struct Biol* **10:**448–454.

Address correspondence to: Dr. Yuji Imaizumi, Department of Molecular and Cellular Pharmacology, Graduate School of Pharmaceutical Sciences, Nagoya City University, 3-1 Tanabedori, Mizuhoku, Nagoya 467-8603. E-Mail: yimaizum@phar.nagoya-cu.ac.jp